scientific reports

Check for updates

OPEN

Evolutionary adaptation of anaerobic and aerobic metabolism to high sulfide and hypoxic hydrothermal vent crab, *Xenograpsus testudinatus*

Chi Chen[1,2]✉, Guan-Chung Wu[1,2]✉, Yung-Che Tseng[3], Sylvie Dufour[2,4] & Ching-Fong Chang[1,2]✉

The vent crab, *Xenograpsus testudinatus* (*xt*crab), is adapted to inhabit shallow-water, high sulfide and hypoxic hydrothermal vent. Our previous study revealed sulfide tolerance of vent *xt*crabs which sulfide: quinone oxidoreductase (*xt*SQR) paralogs aid in sulfide detoxification. However, the mechanisms of how *xt*crab adapts to high sulfide-hypoxic conditions in the vent area remain to be explored. In the present study, we tested the tolerance of *xt*crab to sulfide-induced hypoxia, and investigated their aerobic and anaerobic responses in situ and in the laboratory. Comparisons were made to a non-vent, intertidal species, *Thranita danae* (*td*crab). We analyzed the several factors related to aerobic metabolism (SQR, cytochrome c [CYTC], complex IV [COXIV]), the product of anaerobic metabolism (hemolymph lactate levels) and glucose levels. Our results showed a higher survival tolerance to hypoxia of *xt*crabs than *td*crabs. Hemolymph lactate levels increased more rapidly in *xt*crabs than *td*crabs exposed to experimental hypoxia, revealing a rapid induction of anaerobic metabolism in hypoxic *xt*crabs. Lactate measurement in *xt*crabs returned from aquaria to original capture sites (vent habitats), further assessed the remarkable ability of *xt*crabs to rapidly switch on and off their anaerobic metabolism. To assess aerobic metabolism, long-term exposure of *xt*crabs to hydrothermal vent habitat increased gill *xt*CYTC transcripts and protein levels together with steadily enzymatic activity of COXIV. This revealed ability of *xt*crabs to maintain functional capacity of aerobic respiration in hypoxia. Phylogenetic analysis showed that *xt*SQR paralogs in *xt*crabs were more distant compared to *td*SQR paralogs in *td*crabs. The increase of transcripts and enzymatic activity of gill *xt*SQR, and co-localization of *xt*SQR and *xt*CYTC also contribute to maintain aerobic metabolism by preventing sulfide toxicity on mitochondrial respiratory function. Overall, our study suggests that multiple strategies including detoxification of sulfide by gill *xt*SQR, and a quick/dynamic switch between aerobic and anaerobic metabolisms may play important roles in the metabolic adaptations of *xt*crabs to extreme hydrothermal vent environment.

Keywords Aerobic respiration; anaerobic respiration, Hydrogen sulfide, Cellular energy, Extreme environment, Adaptation

Species living in the intertidal zone and estuaries, such as crustaceans, experience fluctuating oxygen levels[1]. Crustaceans utilize hemocyanin as the primary oxygen-carrying molecule[2]. Generally, crustaceans display a strong tolerance to hypoxic environments by regulating oxygen consumption when ambient O_2 levels decrease[3]. During hypoxia, burrowing crayfish (*Cambarus truncatus*) increase the ventilation rate of the gill[3]. Semiterrestrial crab (*Neohelice granulate*) perform an escape behavior from a hypoxic seawater into tidal zone or land, and also perform anaerobic metabolism with the accumulation of lactate in hemolymph[4,5]. Some species

[1]Department of Aquaculture, National Taiwan Ocean University, Keelung, Taiwan. [2]Center of Excellence for the Oceans, National Taiwan Ocean University, Keelung, Taiwan. [3]Institute of Cellular and Organismic Biology, Academia Sinica, Taipei, Taiwan. [4]Biology of Aquatic Organisms and Ecosystems (BOREA), Muséum National d'Histoire Naturelle, Sorbonne Université, CNRS, IRD, Paris, France. [5]Ching-Fong Chang: Lead contact ✉email: reart002@gmail.com; gcwu@mail.ntou.edu.tw; B0044@email.ntou.edu.tw

like the mediterranean green crab (*Carcinus aestuarii*) can increase the oxygen-binding affinity of hemocyanin during hypoxia[6].

The deep-sea[7] and shallow-water hydrothermal vent environments are characterized by extreme conditions, including high temperatures, high hydrogen sulfide content, low pH, variable oxygen concentrations, and even hypoxia (Table S1). Some species, such as deep-sea vent mussels (*Bathymodiolus thermophilus*) may exhibit a degree of hypoxia tolerance, allowing them to endure fluctuations in oxygen availability and periods of low oxygen in hydrothermal vent environments[8]. Deep-sea hydrothermal vent bivalves (*Gigantidas platifrons*) and shallow-water hydrothermal vent crustaceans (*Xenograpsus testudinatus*) both form symbiotic relationships with chemosynthetic bacteria, which provide a primary source of nutrition through the oxidation of hydrogen sulfide[9,10]. Another deep-sea hydrothermal vent crabs (*Bythograea thermydron*) not only regulates its oxygen consumption rate but also accumulates lactate in hemolymph which indicates the occurrence of anaerobic metabolism[11,12]. Taken together, a hydrothermal vent ecosystem might be considered as a "natural laboratory" to understand versatile physiological adaptations to extreme conditions, particularly high temperature, low pH, high sulfide stress and low oxygen.

The shallow-water hydrothermal vent crabs, *X. testudinatus* (*xt*crab; Xenograpsidae), resides in the hydrothermal vent region of Kueishan Island in Northeastern Taiwan[13]. According to previous studies[14–20] the hydrothermal vent region where vent *xt*crabs reside was characterized by normal seasonal seawater temperatures (20.83–28.09 ℃), lower pH (6–8), lower dissolved oxygen (DO = 4.15–9.5 mg/L), and higher sulfide content (0–3500 μM) (Table S1) compared with the non-hydrothermal vent region around Kueishan Island which exhibited temperatures of 19.93–29.27 ℃, pH 8.01–8.17, DO 7.83–8.29 mg/L, and non-detectable sulfide[14]. Portunidae is a family of crabs that inhabit diverse marine environments, including estuaries, rocky shores, and coral reefs in intertidal and subtidal zones[21]. *Thranita danae* (*td*crab, Portunidae) inhibits the intertidal rocky shore, where variables such as dissolved oxygen, sulfide content (< 300 μM), and pH (6.9–8.3) fluctuate daily[22]. Both *xt*crab and *td*crab inhabit dynamic and variable environments, with the vent conditions being more extreme (Table S1). Studying the physiological differences between *xt*crabs and *td*crabs offers valuable insights on adaptations to extreme environments.

Altered cellular respiration is one of the primary physiological responses to hypoxia. Sulfide decreases the water oxygen content and its toxicity in mitochondrial functions derives the electron from "cytochrome c" resulting in the termination of electron transport chain and the interruption of aerobic respiration[22–25]. Our previous study revealed the presence of duplicated sulfide: quinone oxidoreductase (SQR1 and SQR2) paralogs in vent *xt*crabs[14]. Among them, *xt*SQR1 is predominantly expressed in the gill and showed increased expression in the high-sulfide hydrothermal vent environment, suggesting a specific role in detoxifying environmental sulfide into less toxic compounds.[14] We propose that acclimation to high-sulfide hydrothermal vent environments is partly facilitated by duplicated SQR paralogs in *xt*crabs, which may function in sulfide detoxification and support aerobic metabolism. However, our understanding of the respective aerobic and anaerobic pathways in the *xt*crabs under the sulfide-rich and hypoxic hydrothermal vent environment remains limited.

In this study, we hypothesized the importance of switching between aerobic and anaerobic metabolism, as part of the metabolic adaptation of *xt*crabs in response to high sulfide stress and serve hypoxia. We measured the hemolymph lactate levels in *xt*crabs and *td*crabs, which is considered an indicator of anaerobic metabolism. To examine aerobic metabolism, we focused on cytochrome c (CYTC), a highly conserved protein that plays a crucial role in cellular respiration. Cytochrome c is primarily involved in the mitochondrial electron transport chain, where it shuttles electrons between Complexes III and IV, to facilitate the production of ATP[26]. We measured gill levels of CYTC transcripts and of mitochondiral Complex IV (COXIV, also named cytochrome c oxidase) enzymatic activity, as indicators of aerobic metabolism. In addition, we also measured transcript levels and enzymatic activity of gill SQR as the facilitative factor for aerobic metabolism and removal of sulfide toxicity in high sulfide environment. The survival of *xt*crabs in hypoxia and their metabolic responses were tested through laboratory experiments. Comparisons were made with a non-vent, intertidal crab species, *td*crab. The phylogenetic relationship between *xt*SQR paralogs and *td*SQR paralogs was further compared. Most importantly we performed field studies, including transferring *xt*crabs from the hydrothermal vent habitat to normal seawater aquarium, or conversely transfer of normal seawater acclimated *xt*crabs to the hydrothermal vent region or the non-hydrothermal vent region of Kueishan Island.

Results

Hypoxic tolerance

All aquarium *xt*crabs exhibited the activities and survived under hypoxia (DO = 0.19 mg/L) up to 16 h. All control species *td*crabs exhibited the activities and survived only up to 8 h (Fig. 1a). Meanwhile, all *xt*crabs and *td*crabs survived in normoxia seawater for 24 h (data not shown). These data demonstrated that vent *xt*crabs tolerated hypoxic stress greater than intertidal *td*crabs.

Antimycin A is a potent inhibitor of mitochondria by interrupting the electron transport chain[27,28]. Antimycin A was used to induce the cellular hypoxia in *xt*crabs with various concentrations (up to 1000 ppb) for 96 h (Fig. 1b). All *xt*crabs survived in 0, 1, and 10 ppb treatments up to 96 h, but the survival rates decreased with the increase of antimycin A concentrations (100, 500, and 1000 ppb) and exposure time (up to 96 h), showing dose-dependent decreasing survivals. Based on the survival rates and their relative concentrations of antimycin A, we estimated the LC_{50}/96 hr was 265 ppb in *xt*crabs (Fig. 1b).

To further assess the effects of antimycin A in *xt*crabs, oxygen consumption rate was measured to validate the interference to the aerobic respiration of *xt*crabs under antimycin A treatments for the durations of 30 min. The oxygen consumption rate was significantly decreased in the 400 ppb group (0.28 ± 0.08 mg O_2 g^{-1} hr^{-1}) compared to the 0 ppb group (0.70 ± 0.14 mg O_2 g^{-1} hr^{-1}; $p < 0.05$; Fig. 1c). The oxygen water content of the 0 ppb group decreased faster within 30 min (Fig. 1d) compared to the oxygen water content of the 400 ppb group

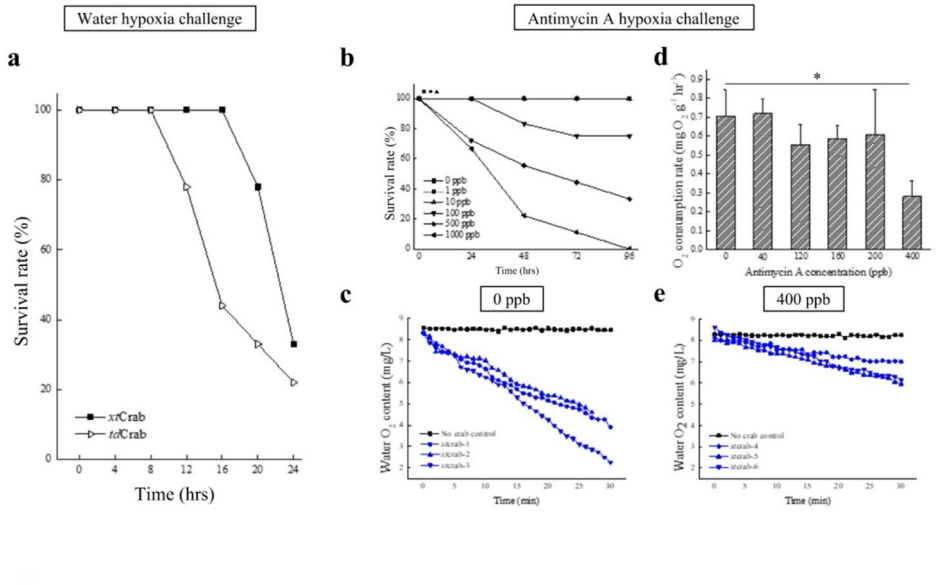

Fig. 1. Survival of hypoxia and antimycin A challenge in the hydrothermal vent *xt*crabs. (**a**) Aquarium *xt*Crabs (*Xenograpsus testudinatus*) and control *td*crabs (*Thranita danae*) collected from their original habitats (hydrothermal vent and intertidal zone, respectively) were maintained for one month in the normal seawater aquarium for acclimation. Then aquarium *xt*crabs and control *td*crabs were subjected to a severe hypoxic challenge (Dissolved oxygen, DO = 0.19 mg/L seawater continuously flushed with nitrogen gas. DO of the normoxia group = 8.31 mg/L). The activity levels of *xt*crabs and *td*crabs, including movement, touching reaction, and body calibration were checked every 4 h over 24 h period ($n = 9$ crabs/group). (**b**) LC_{50}/96 hr of antimycin A was tested in aquarium *xt*crabs. The aquarium *xt*crabs were exposed to various antimycin A concentrations (0 ppb, 1 ppb, 10 ppb, 100 ppb, 500 ppb, 1000 ppb) for 96 h. Survival was recorded every 24 h for each group ($n = 9$ *xt*crabs/group). (**c**) Oxygen consumption rate (mg O_2 g^{-1} hr^{-1}) in *xt*crab under different antimycin A treatments for 30 min were examined. Means ± SD ($n = 3$ *xt*crabs/group). Asterisks indicate the significant difference between 0 ppb and 400 ppb group by *t*-test (*: $p < 0.05$). (**d**) Oxygen content in a sealed water chamber for each *xt*crab was recorded under 0 ppb antimycin A treatment for 30 min. (**e**) Oxygen content in a sealed water chamber for each *xt*crab was recorded under 400 ppb antimycin A treatment for 30 min.

(Fig. 1e), illustrating that antimycin A could interrupt the mitochondrial electron transport chain in *xt*crabs. Taken together, these data showed that *xt*crabs had a higher tolerance to severe hypoxic environments than control *td*crabs.

Regulation of lactate level under various environmental conditions

The results of 12 h hypoxia challenge showed that the lactate level observed in *xt*crabs were significantly increased in 1 h (10-fold, $p < 0.001$), 3 h (108-fold, $p < 0.001$), 6 h (146-fold, $p < 0.001$), and 12 h (144-fold, $p < 0.001$) compared to 0 h of immersion in hypoxic seawater (Fig. 2a). In contrast, the lactate level observed in *td*crabs were significantly increased only after 12 h (7.8-fold, $p < 0.001$; Fig. 2b).

To investigate that sulfide-rich hydrothermal vent environments would induce the anaerobic metabolism to *xt*crabs, habitat *xt*crabs were immersed in sulfide-free normal seawater for different time periods. The results showed that the lactate level was significantly decreased in the 30 min group, then dramatically dropped in the 60 min group, and remained constant in the 6 h, 12 h, and 1 month groups ($p < 0.05$; Fig. 2c). Lab-maintained aquarium *xt*crabs were transferred back to sea for 2 h either in the hydrothermal vent sulfide-rich seawater environment (station-1 *xt*crabs; Fig. 3; Table S1) or normal seawater environment (station-2 *xt*crabs; Fig. 3). The lactate level in hemolymph samples were significantly higher in habitat *xt*crabs and station-1 *xt*crabs while not in station-2 *xt*crabs and aquarium *xt*crabs ($p < 0.05$; Fig. 2d). These results revealed that the increased lactate levels in hemolymph clearly indicate the crabs were exposed to the hypoxic environment. Furthermore, under hypoxic or hydrothermal vent environments, anaerobic metabolism rapidly switched on within 1 h in *xt*crabs.

Regulation of glucose level under various environmental conditions

In the immersion of hypoxia experiment, the glucose level of *xt*crabs was significantly decreased in 3 h compared to 0 h ($p < 0.05$), but returned to initial levels at 6 h and 12 h (Fig. S1a) while the glucose level of *td*crabs showed no significant difference among groups ($p > 0.05$; Fig. S1b). In the experiment of habitat *xt*crabs transferred to sulfide-free normal seawater, the glucose level of *xt*crabs in each group showed no significant difference ($p < 0.05$; Fig. S1c). In the immersion of hydrothermal vent, station-1 and station-2 experiment, the glucose level of *xt*crabs showed no significant difference ($p > 0.05$; Fig. S1d). Overall, glucose level showed no change and remained

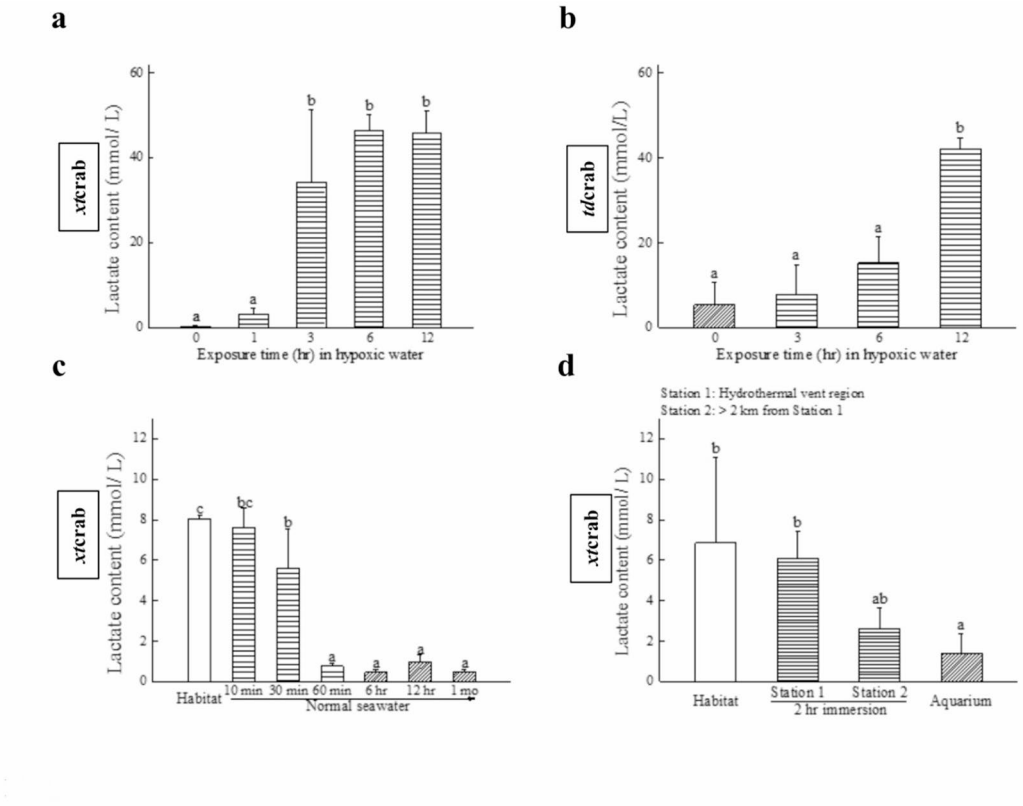

Fig. 2. Lactate levels in hemolymph under vent habitat, non-vent aquarium, and hypoxia environment in the *xt*crabs. To study the effects of severe hypoxic environments on respiration metabolism, aquarium *xt*crabs and control *td*crabs were immersed in the nitrogen gas-induced severe hypoxic seawater (DO = 0.19 mg/L) for 12 h, respectively. During 12 h of severe hypoxic seawater exposure, hemolymph samples were collected at 0, 1, 3, 6, and 12 h ($n = 8$ *xt*crabs/group; $n = 4$ *td*crabs/group). (**a**) Lactate levels in hemolymph of *xt*crabs under severe hypoxia for different periods. (**b**) Lactate levels in hemolymph of *td*crabs under severe hypoxia for different periods. To investigate the respiration metabolism of hydrothermal vent in *xt*crabs, habitat *xt*crabs transferred to normal seawater on the boat and then transferred to the lab aquarium. Hemolymph samples were collected for several intervals including habitat *xt*crabs, transferred habitat *xt*crabs immersed in normal seawater for 10 min, 30 min, 60 min, 6 h, 12 h, and 1 month ($n = 4$ *xt*crab/group). (**c**) Lactate levels in hemolymph of habitat *xt*crabs transferred to normal seawater for different periods. To further investigate the effects of hydrothermal vent environments on respiration metabolism, aquarium *xt*crabs were transferred to station-1 (hydrothermal vent region, station-1 *xt*crabs) or station-2 (sulfide-free region with normal seawater, station-2 *xt*crabs) for 2 h with cages. After transfer, hemolymph samples were obtained immediately on the boat. Meanwhile, hemolymph samples of habitat *xt*crabs and aquarium *xt*crabs (0 point) were also collected on the boat for further comparison ($n = 8$ *xt*crab/group). (**d**) Comparison of lactate levels in hemolymph among different *xt*crabs of habitat *xt*crabs, aquarium *xt*crabs, station-1 *xt*crabs, and station-2 *xt*crabs. Different letters indicate significant differences among groups by one-way ANOVA ($p < 0.05$). Asterisks indicate significant difference between groups by *t*-test (*: $p < 0.05$; **: $p < 0.01$; ***: $p < 0.001$). The bar represents mean ± SD (standard deviation).

stable in all experiments. Taken together, these indicate that *xt*crabs are able to maintain constant hemolymph glucose levels under hypoxic or hydrothermal vent environments.

Molecular identification of *xt*crab CYTC and development of *xt*CYTC qPCR analysis

De novo assembly of our on-going draft transcriptomic database (SRR33664475) and BLAST search using human *CYTC* (PV554173) allowed us to obtain a potential *CYTC* sequence in *xt*crabs. Using the specific primers designed from the potential *CYTC* sequence, we identified and cloned one *CYTC* sequence, named *xtCYTC*, from the gill of *xt*crabs. The results of phylogenetic analysis showed that *xt*CYTC was clustered with other CYTC sequences from crustaceans (Fig. S2). To develop *xtCYTC* quantitative real-time PCR (qPCR) analysis, specific qPCR primers were designed and applied for qPCR reactions (Table S2). After the qPCR reaction, the amplified products of the *xtCYTC* DNA were sequenced, which confirmed the specificity of the *xtCYTC* qPCR primers.

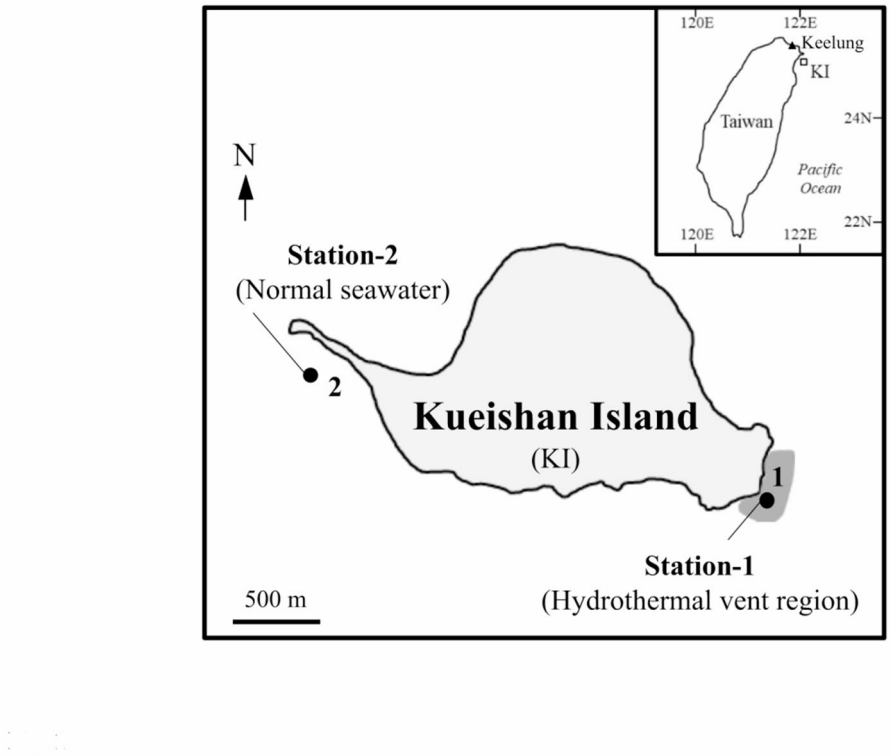

Fig. 3. Location for the collection of vent *xt*crabs off Kueishan Island in the Northeast of Taiwan. The habitat for *xt*crabs of shallow-water hydrothermal vents is located on the Southeast of Kueishan Island (Northeastern Taiwan) at a depth of about 10–20 m (station-1; 24°50′31″N, 121°57′6″E). In contrast, no hydrothermal vent is present on the other side of the island (station-2; 24°50′558″N, 121°56′212″E). With the advantages of these unique environments, we can collect *xt*crabs from their habitat (habitat *xt*crabs) and culture them at the lab aquarium for at least 1 month (aquarium *xt*crabs). For the field transfer experiment, the aquarium *xt*crabs were transferred to the hydrothermal vent environments station-1 (station-1 *xt*crabs) or station-2 with sulfide-free normal seawater (station-2 *xt*crabs) for further comparison. For comparison, we collect control *td*crab from intertidal habitat (Keelung coast, 25°08′09.1″N, 121°48′10.4″E) and culture at the lab aquarium for at least 1 month (control *td*crabs). White square indicates the habitat for *xt*crabs (KI, Kueishan Island). Black triangle indicates the habitat for *td*crabs (Keelung).

Tissue distribution of *xt*CYTC transcripts and regulation of *xt*CYTC transcripts, *xt*CYTC protein level, and COXIV enzymatic activity by high sulfide-hypoxia environment

An upregulation of CYTC expression was observed in the posterior gill (pGi), which showed a significant increase in habitat *xt*crabs compared to that in aquarium *xt*crabs (6.7-fold, $p < 0.05$) (Fig. 4a). To further investigate the potential correlation between the expression of *xtCYTC* transcripts in pGi and the high sulfide-hypoxia hydrothermal vent environment, the results of *xtCYTC* transcripts in gills showed a significant increase in the habitat *xt*crabs compared to that in the aquarium *xt*crabs (2.6-folds, $p < 0.001$; Fig. 4b).

The specificity of anti-*xt*CYTC was confirmed by a Western blot (WB) analysis with peptide preadsorption (Fig. S3). WB with anti-*xt*CYTC showed a major band of approximately 12 kDa, which is in agreement with the predicted molecular size (Fig. S3). Moreover, the absent immunoblot signal of CYTC was observed using the preadsorbed antisera (Fig. S3). These data suggested that the polyclonal antisera of anti-*xt*CYTC successfully identified the CYTC protein in *xt*crabs. To compare the patterns of *xt*CYTC protein expression between habitat *xt*crabs and aquarium *xt*crabs, the immunoblot signal was significantly increased in habitat *xt*crabs compared to the aquarium *xt*crabs group ($p < 0.05$; Fig. 4c). After normalizing the *xt*CYTC signals to Actin levels, the habitat *xt*crabs exhibited 6.8-fold higher gill expression of *xt*CYTC protein compared to the aquarium group (Fig. 4c). Original complete blots and multiple brightness of WB analysis (Fig. S4a-4c) demonstrated the valid of the data. *xt*COXIV activity analysis showed no significant difference between the habitat *xt*crabs and aquarium *xt*crabs ($p > 0.05$; Fig. 4d).

Molecular identification of *xt*crab SQR paralogs, *td*crab SQR paralogs, and phylogenetic analysis

Our previous study obtained the full coding DNA sequence (CDS) of *xt*crabs and further demonstrated that the expression of duplicated and subfunctionalized SQRs is strongly up-regulated by hydrothermal vent environments in *xt*crabs[14]. For further comparison of SQRs between vent *xt*crabs and control *td*crabs, the full CDS of *tdSQR*paralogs was obtained. According to previous studies[29,30] we annotated three putative FAD-

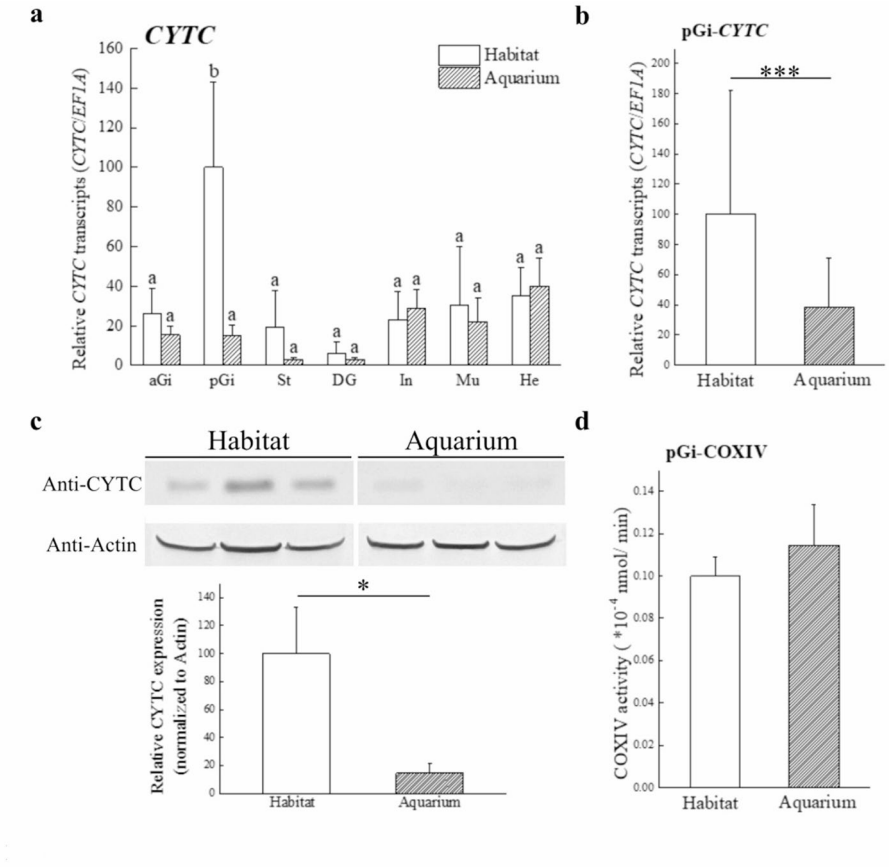

Fig. 4. *xtCYTC* transcripts, *xt*CYTC protein, and *xt*COXIV enzymatic activity expressions under various environments. (**a**) Tissue distribution of *xtCYTC* transcripts in various tissues collected from habitat *xt*crabs and aquarium *xt*crabs ($n = 6$ crabs/group). aGi, anterior gill; pGi, posterior gill; St, stomach; DG, digestive gland; In, intestine; Mu, muscle; He, heart. (**b**) *xtCYTC* transcripts in pGi of habitat *xt*crabs and aquarium *xt*crabs ($n = 36$ crabs/group). (**c**) *xt*CYTC protein expression as measured by Western blot (with *xt*CYTC antiserum) in the pGi of habitat and aquarium *xt*crabs. Selected blot images are depicted above the graphs. Actin was used as a reference protein. Quantification of signal intensity was performed with ImageJ software ($n = 3$ *xt*crabs/group). (**d**) COXIV enzymatic activity in habitat *xt*crabs and aquarium *xt*crabs ($n = 6$ crabs/group). Different letters indicate one-way ANOVA in *xt*CYTC tissue distribution ($p < 0.05$). *EF1A* was used as an internal reference to normalize the gene expression levels. The highest value among groups is set at 100, and each value is normalized to the ratio (each value/highest value) x100. Asterisks indicate significant difference between groups by *t*-test (*: $p < 0.05$; **: $p < 0.01$; ***: $p < 0.001$). The bars represent mean ± SD (standar deviation).

binding domains (I, II, and III), one sulfide oxidation domain, and one quinone reduction domain in the SQR sequences of *xt*crabs and *td*crabs (Fig. S5a). The identity of *xt*SQR1 and *xt*SQR2 was 86.36%, and the identity of *td*SQR1 and *td*SQR2 was 92.48% (Fig. S5b). These data suggest that *xt*SQR1 and *xt*SQR2 paralogs were more divergent compared to *td*SQR1 and *td*SQR2 paralogs.

To investigate the phylogenetic relationships between *xt*SQR paralogs and *td*SQR paralogs, the partial sequences of cp.SQR paralogs (*Cancer pagurus*, cp.SQR1 and cp.SQR2) and *es*SQR (*Eriocheir sinensis*), the full-length sequences of *xt*SQR paralogs[14] and *td*SQR paralogs were used together with other SQR sequences of metazoan species from the NCBI database for the phylogenetic analysis. The phylogenetic analysis showed that *xt*SQR paralogs and *td*SQR paralogs clustered with SQR sequences from crustaceans (Fig. 5a). About 36% species of crustaceans (4 species from 11 total species) had duplicated SQR paralogs. In contrast, there is no SQR duplication occurred in vertebrates and other invertebrates (Fig. 5a). Among the crab SQR sequences, the *xt*SQR1 and *xt*SQR2 in *xt*crabs were quite distant in the phylogeny tree; while *td*SQR1 *vs.* *td*SQR2 in *td*crabs, *cb*SQR1 *vs.* *cb*SQR2, and cp.SQR1 *vs.* *cp.*SQR2 in other crustaceans were clustered more closely (Fig. 5a). Moreover, both *xt*SQR paralogs and *td*SQR paralogs did not cluster with the *Cancer borealis*/*C. pagurus* SQR paralogs (Fig. 5a).

Regulation of *xt*SQR1 transcripts and comparison of SQR enzymatic activity between *xt*crabs and *td*crabs

qPCR results showed that *xtSQR1* transcripts in gills were significantly increased in the habitat *xt*crabs compared to that in the aquarium *xt*crabs ($p < 0.05$; Fig. 5b). SQR enzymatic activity was also significantly higher in habitat

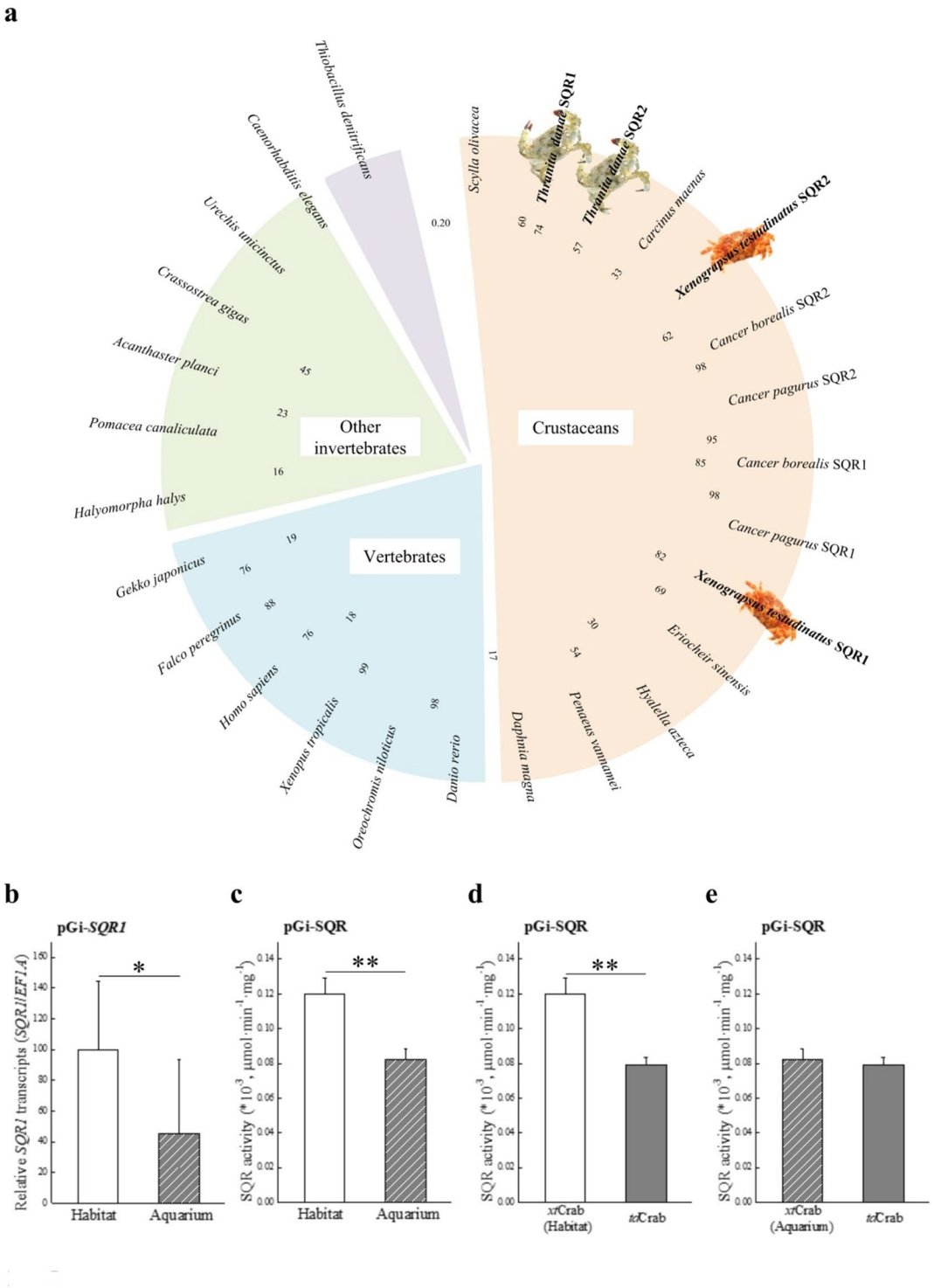

Fig. 5. Multidisciplinary investigations of SQR from sequences to enzymes. (**a**) Phylogenetic analysis of SQR amino-acid sequences from various species. SQR sequences of *xt*crab and *td*crab were marked with the bottom line. Numbers indicate bootstrap values (% of 1000 replicates). pGi samples collected from habitat *xt*crabs and aquarium *xt*crabswere used for the analysis of *xtSQR1* transcripts and SQR enzymatic activity. (**b**) *xtSQR1* transcripts in pGi of habitat *xt*crabs and aquarium *xt*crabs ($n = 10$ *xt*crabs/group). (**c**) SQR enzymatic activity of pGi in habitat *xt*crabs and aquarium *xt*crabs ($n = 3$ crabs/group). (**d**) SQR enzymatic activity in habitat *xt*crabs and *td*crabs. (e) SQR enzymatic activity in aquarium *xt*crabs and *td*crabs ($n = 3$ crabs/group). *EF1A* was used as an internal reference to normalize the gene expression levels. The highest value among groups is set at 100, and each value is normalized to the ratio (each value/highest value) x100. Asterisks indicate significant difference between groups by *t*-test (**: $p < 0.01$; ***: $p < 0.001$). The bar represents mean ± SD (standard deviation).

*xt*crabs compared to that in the aquarium *xt*crabs ($p < 0.01$; Fig. 5c). These data also agree with our previous study that the high sulfide-hypoxia hydrothermal vent environment would up-regulate the SQR expression level (transcripts and protein)[14].

SQR enzymatic activity showed a significantly higher level in habitat *xt*crab compared to control *td*crab (1.5-fold, $p < 0.01$; Fig. 5d). Moreover, SQR enzymatic activity showed no significant difference between aquarium *xt*crabs and control *td*crabs ($p > 0.05$; Fig. 5e). These data further support the strong ability of vent *xt*crabs to up-regulate of gill *xt*SQR enzymatic activity in the face of sulfide-rich vent environment.

The localization of *xt*CYTC and *xt*SQR-expression cells in in *xt*crab gills

Bright field vision under microscopy with DAPI nuclei staining showed the structure of gill filaments (Fig. 6a). NKA-antibody was used to annotate the basolateral membranes of pillar cells (Fig. 6b and e) as previous studies[14,31]. Cytoplasm of pillar cells and hemocytes in the gill filament exhibited detectable levels of *xt*SQR (Fig. 6c and e, and 6f) and *xt*CYTC (Fig. 6d and f). Notably, except for the absence of NAK signal in hemocytes, all hemocytes expressed *xt*SQR and *xt*CYTC, and all pillar cells expressed NKA, *xt*SQR, and *xt*CYTC, according to sections that were co-stained with DAPI-SQR-NKA (Fig. 6e) and DAPI-SQR-CYTC (Fig. 6f). Remarkably, we found co-localization of *xt*SQR and *xt*CYTC in each of more than 100 SQR-positive cells examined from six *xt*crabs.

Discussion

For the acclimation of a hypoxia environment, several strategies have been evolved in crustaceans, such as avoidance behaviors to escape from the hypoxic environment, increasing gill ventilation rates, adjusting the oxygen affinity of hemocyanin, and the onset of anaerobiosis, as evidenced by increased hemolymph lactate levels[3–6].

Here, we focused on the aerobic and anaerobic metabolism for the *xt*crabs adapted to the hydrothermal vent extreme environment. With the comprehensive approaches including biochemical, molecular, and enzymatic analyses, our findings revealed that the rapid activation of anaerobic metabolism and the maintenance of aerobic metabolism simultaneously occurred in vent *xt*crabs. We combined the favorable factors for aerobic respiration, including *xt*SQR and *xt*CYTC, with lactate, a major end product of anaerobic respiration. Our results demonstrated that these biochemical parameters (*xt*SQR and *xt*CYTC) were strongly up-regulated by the hydrothermal vent environment.

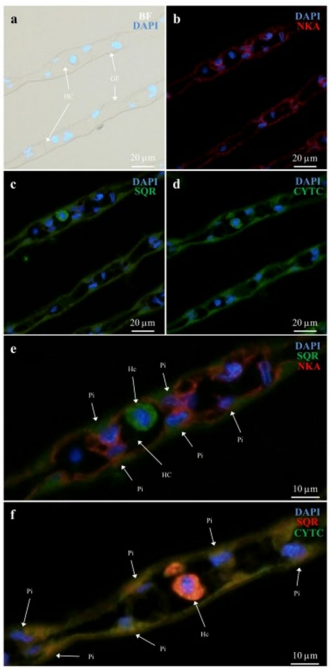

Fig. 6. The localization of *xt*CYTC-expression cells in the gills. (**a**) Bright Field under microscopy and cell nuclei staining with DAPI (4', 6-diamidino-2-phenylindole; blue) were used for the observation of gill structure. (**b**) Immunofluorescence staining with NA^+/K^+-ATPase (NKA) antibody was performed to localize NKA (red) expression in the gill. (**c**) Immunofluorescence staining with *xt*SQR antibody was performed to localize *xt*SQR (green) expression in the gill. (**d**) Immunofluorescence staining with *xt*CYTC antisera was performed to localize *xt*CYTC (green) expression in the gill. (**e**) The DAPI (blue), *xt*SQR (green), and NKA (red) merged figure showed the co-localization of *xt*SQR and NKA signals in the gill. (**f**) The DAPI (blue), *xt*SQR (red), and *xt*CYTC (green) merged figure showed the co-localization of *xt*SQR and *xt*CYTC signals in the gill. HC: hemal channel; GF: gill filament; Hc: hemocyte; Pi: pillar cell. ($n = 6$ *xt*crabs).

We examined the hypoxia tolerance of aquarium *xt*crabs and control *td*crabs exposed to hypoxia in aquaria (DO = 0.19 mg/L seawater continuously flushed with nitrogen gas). All *xt*crabs and *td*crabs exposed to the hypoxic condition survived at least 8 h of exposure, and both species exhibited routine behaviors. However, the *xt*crabs showed greater ability to tolerate severe hypoxia compared to *td*crabs. Following 16 h of hypoxic exposure, the *xt*crabs fully survived in the hypoxic condition, while *td*crabs experienced mass mortality. This suggests that the *xt*crabs possessed specialized physiological acclimations to prolonged severe hypoxia. Generally, environmental hypoxia refers to the phenomenon where the concentration of dissolved oxygen in marine and estuarine waters is below 2–3 mg/L and in freshwater below 5–6 mg/L, while severe hypoxia is defined as ≤ 0.5 mg/L[32,33]. Our previous study recorded that the dissolved oxygen levels ranged from 4 to 7 mg/L in the hydrothermal vent region of Kueishan Island[14]. The dissolved oxygen levels in the habitat of the deep-sea hydrothermal vent crab, *Bythograea thermydron*, were recorded to range from 0 to 1.76 mg/L[34]. According to our present data, vent *xt*crabs could survive in the severe hypoxic environment.

Antimycin A is a fungal resource-metabolites of mixture, which is the inhibitor of the mitochondrial electron transport chain, and widely used as a piscicide to control the fish populations in USA[27,28,35]. We examined the antimycin A tolerance and confirmed the LC_{50}/96 hr was 265 ppb in aquarium *xt*crabs. Our findings also revealed that antimycin A reduced the oxygen consumption rates in *xt*crabs, suggesting that aerobic electron transport was inhibited under antimycin A treatment. Previous studies recorded the LC_{50}/96 hr of antimycin A in various species including American paddlefish (*Polyodon spathula*, 0.0017 ppb), rainbow trout (*Oncorhynchus mykiss*, 0.04 ppb), black bullhead catfish (*Ameiurus melas*, 45 ppb), and a freshwater amphipod (*Gammarus fasciatus*, 0.0089 ppb)[36,37]. This suggests that *xt*crabs have well-developed underpinning cellular mechanisms to tolerate hypoxia, caused by the ambient hypoxic water and cellular hypoxia induced by an inhibitor of electron transport chain.

To understand the alternation of aerobic and anaerobic metabolism in hypoxic environments, the hemolymph lactate, the end product of the anaerobic metabolism, was measured. Aquarium *xt*crabs and control *td*crabs were immersed in severe hypoxic seawater (DO = 0.19 mg/L) for 12 h. Both *xt*crabs and *td*crabs showed increased lactate content in hemolymph. However, unlike the rapid increase in *xt*crabs (1 h), the lactate level showed a significant increase until 12 h in hemolymph of *td*crabs. These data demonstrated that *xt*crabs showed a faster activation of anaerobic respiration than *td*crabs. Our field study showed higher lactate level in habitat *xt*crab (6.9 ± 4.2 mmol/L), which have a long term exposure to hydrothermal vent environment, as compared to aquarium *xt*crab exposed for one month to normal sea water (1.9 ± 1.0 mmol/L). Furthermore, the time course of the decrease in lactate levels after transfer of habitat *xt*crab to normal sea water on the boat, showed a rapid drop already significant after 30 min of transfer. This further highlights the ability of *xt*crab to rapidly switch on and off their anaerobic metabolism. Little information is available for the lactate accumulation in the crabs. Anaerobic metabolism is also known to occur along with the accumulation of lactate during prolonged exercise in *Necora puber* crabs[38]. In the deep-sea hydrothermal vent crabs (*B. thermydron*), lactate accumulation was found to occur in the hydrothermal vent environment[12]. Previous study revealed that vent *xt*crabs under acidified conditions (pH 6.5) dropped hemolymph pH unit by 0.25 compared to control (pH 8.0) but hemolymph pH value could restore after 4 h and then stably maintained to pH 7.4. Meanwhile, gill Na^+/K^+-ATPase (NKA) and V-type H^+-ATPase (VHA), the primary ion pumps responsible for acid–base regulation, exhibited marked upregulation at the mRNA, protein, and enzymatic activity levels under acidified conditions[31]. We postulate that well-developed gill machinery associated with ion transport and acid-base regulation may help buffer their extracellular pH during the onset of anaerobiosis and an accumulation of hemolymph lactate[31]. This mechanism may imply that *xt*crabs have much more capacity for lactate accumulation in hemolymph. The possible excretion of lactate *via* gill, mucus, or other organs to alleviate the lactate burden could not be excluded. Taken together, the rapid switch-on of the anaerobic metabolism and strong ion regulatory ability in vent *xt*crabs may help them conquer the hypoxic environment. Moreover, these data suggest that the high sulfide-hypoxia hydrothermal vent environment in Kueishan Island may induce a rapid switch on anaerobic metabolism in *xt*crabs.

Previous studies have reported that hypoxia triggers the activation of gluconeogenesis to maintain aerobic metabolism in various crustacean species[39,40]. In Chinese mitten crab (*Eriocheir sinensis*) and Chinese grass shrimp (*Palaemonetes sinensis*), previous study revealed that a significant increase in glucose content after environmental hypoxia[41]. However, the glucose content in vent *xt*crabs showed no significant difference after severe hypoxia exposure or the field transfer experiment. Glucose serves as the primary energy source for both aerobic and anaerobic metabolism[42]. Additionally, glucose is synthesized from the end products of anaerobic metabolism, such as lactate, to facilitate recovery after hypoxia[43]. Our findings suggest that the pathways to maintain glucose supply are well operated under energy-demanding conditions and also the increase of lactate could be the indicator for the experience of hypoxia in *xt*crabs. Moreover, in the extreme environment of a hydrothermal vent and at the limits of hypoxia, aerobic and anaerobic metabolism may simultaneously occur and dynamically switch on and off in vent *xt*crabs, depending on the concentrations of environmental sulfide and dissolved oxygen. *xt*Crabs have the strong ability to rapidly turn on the anaerobic metabolism for the supply of metabolic energy. Therefore, maintaining glucose supply and rapidly activating anaerobic metabolism are suggested as the potential strategies for survival and adaptation in vent *xt*crabs to the high sulfide-hypoxic extreme environment.

In the present study, we cloned the full-ORF of two *SQR* gene paralogs from *td*crabs (*td*SQR1 and *td*SQR2). Both *td*SQR1 and *td*SQR2 performed the functional domains as conserved SQR. The phylogenetic analysis exhibited that *td*SQR1 and *td*SQR2, and other paralogs were clustered more closely, while *xt*SQR1 and *xt*SQR2 were quite distant. These findings further support the occurrence of SQR duplication and subfunctionalization in vent *xt*crabs as suggested in our previous study[14]. We also revealed that several independent SQR duplication events occurred across the brachyuran lineage but not in other metazoans[14]. The independent SQR duplication in *td*crabs and *xt*crabs suggested a potential impact on the fate of gene mutations. We proposed that the high

H_2S hydrothermal vent extreme environment might be one of the factors driving the duplication and further subfunctionalization of SQR in vent *xt*crabs.

Again, we confirm the sulfide detoxification ability of SQR in vent *xt*crabs. The increase of *xtSQR1* transcripts/protein and *xt*SQR enzymatic activity in habitat *xt*crabs also agrees with our previous study[14]. To clarify the *xt*SQR ability in *xt*crabs, intertidal *td*crabs was used as a control species for the comparison of enzymatic activity. SQR activity were significantly increased in habitat *xt*crabs compared to aquarium *xt*crabs and control *td*crabs. In aquarium *xt*crabs, no difference in SQR enzymatic activity was observed between aquarium *xt*crabs and *td*crabs. These data highlight the strong ability and high plasticity of *xt*SQR in *xt*crabs under high sulfide hydrothermal vent environment.

Sulfide can inhibit mitochondrial cytochrome c oxidase activity by blocking the electron transport chain in animals[44]. High concentrations of sulfide decreased the reduction state of CYTC (become oxidized CYTC state) and dissolved oxygen, and further resulted in the termination of aerobic respiration[24,25]. Mitochondrial respiratory chain is suggested to be critical for the adaptation to the exposure to hydrogen sulfide and sulfide detoxification mediated by SQR[45]. Therefore, high *xt*SQR expressions at gene and enzyme levels also help mitochondria to maintain the electron transport chain to further facilitate the activity of aerobic metabolism. Moreover, in short-term acclimation, there might be other potential strategies to overcome sulfide toxicity and hypoxia, such as temporary alternation to anaerobic metabolism to achieve the energy demand.

In the present study, we identified and cloned *CYTC* gene from *xt*crabs. Our phylogenetic analysis showed that *xt*CYTC was clustered with CYTC from other crustacean. According to our qPCR results, *xtCYTC* was expressed in all investigated tissues of habitat *xt*crabs and aquarium *xt*crabs, including anterior gill, posterior gill, stomach, digestive gland, intestine, muscle, and heart, but it showed a significant increase specifically in the posterior gill of habitat *xt*crabs. Gills are the major respiratory organs in aquatic crustaceans that perform essential functions in ion transport and osmoregulation[46]. Cytochrome c, which plays a crucial role in aerobic metabolism, is an electron carrier between Complex III (cytochrome bc1 complex) and Complex IV (cytochrome c oxidase) in the mitochondrial inner membrane to maintain the electron transport chain[47]. However, the electron transport chain would be interrupted by surrounding sulfide *via* the deprivation of electron from reduced CYTC[23–25]. As the sulfide detoxification-related *xt*SQR paralog we revealed in our previous study, *xt*CYTC also showed upregulation in the high sulfide vent environment. An increase in *CYTC*, which is associated with a significant increase in cellular respiration, has been confirmed in mouse embryonic fibroblasts under serum starvation up to 12 h[48].

To further evaluate the contribution of aerobic respiration in the gill of habitat *xt*crabs and aquarium *xt*crabs, *xt*COXIV enzymatic activity was conducted. The results of *xt*COXIV enzymatic activity showed that habitat *xt*crabs under extreme environment had a similar activity to aquarium *xt*crabs. Previous study revealed that COXIV enzymatic activity was reduced under hypoxic conditions (DO = 2 mg/L for 6 h), and gradually increased as hypoxia continued (DO = 1 mg/L for another 6 h) in white shrimp (*Litopenaeus vannamei*)[49]. This evidence suggested that the shortage of oxygen would inhibit the activity of aerobic metabolism in crustaceans. Unlike crustaceans, the shortfin molly (*Poecilia Mexicana*), which lived in the sulfide-spring region, evolved a lower H_2S susceptibility of COX to adapt the sulfide environment[50]. These data suggested that *xt*crabs are able to maintain aerobic metabolism even in the high sulfide and hypoxic hydrothermal vent environment. Altogether, we hypothesize that the increased expression *xtCYTC* (transcripts and protein) may compensate the reduction of CYTC activity due to hypoxia and sulfide-induced oxidized *xt*CYTC to maintain the *xt*COXIV function for the electron transport chain and aerobic metabolism.

In *xt*crab, CYTC expression was observed in all hemocytes and pillar cells of the gill filament. Here, we also established the SQR antibody against the *xt*SQR in *xt*crab. Impressively, all observed *xt*CYTC-positive cells were also *xt*SQR-positive cells and all observed *xt*SQR-positive cells were also NKA-positive cells. Our previous study demonstrated the co-localization of SQR and NKA in pillar cells using anti-human SQR[14], which agreed with our results in the present study with anti-*xt*SQR antibody. We also confirmed the localization of *xt*SQR in the mitochondria by protein fraction analysis[14]. In mammalian cells, CYTC, which serves as the electron carrier protein, is localized in the mitochondria[26,51]. Higher protein level and enzymatic activity of *xt*SQR (in previous[14] and the present study) and protein level of *xt*CYTC (the present study) were found in the vent habitat *xt*crabs as compared to the aquarium *xt*crabs. Hence, we proposed that the sulfide detoxification *via* SQR might prevent CYTC from electron deprivation. Moreover, the production of electrons during sulfide detoxification might be recruited to the electron pool in the mitochondrial electron transport chain. These proposed mechanisms may be favorable factors for the maintenance of aerobic metabolism in *xt*crabs under the sulfide-hypoxia hydrothermal vent environment.

Conclusion

Our study revealed metabolic strategies that enable the hydrothermal vent crab *X. testudinatus* to tolerate hypoxic and sulfide-rich conditions. The mechanisms for the physiological adaptation of *xt*crabs to high sulfide and low dissolved oxygen in hydrothermal vents were proposed (Fig. 7). The rapid increase in hemolymph lactate levels during hypoxic exposure indicates the rapid activation of anaerobic metabolism, helping the crab endure oxygen depletion—an important physiological adaptation to vent environments. Both low oxygen and high sulfide inhibit aerobic metabolism by reducing CYTC activity and disrupting electron transfer in the electron transport chain. However, the long-term increase of gill *xt*CYTC expression in vent-adapted *xt*crabs may compensate for sulfide inhibition. The maintained enzymatic activity of *xt*COXIV, together with high expressions of *xt*SQR and *xt*CYTC, and their cellular co-localization, might support the persistence of aerobic respiration for energy production in the vent habitat.

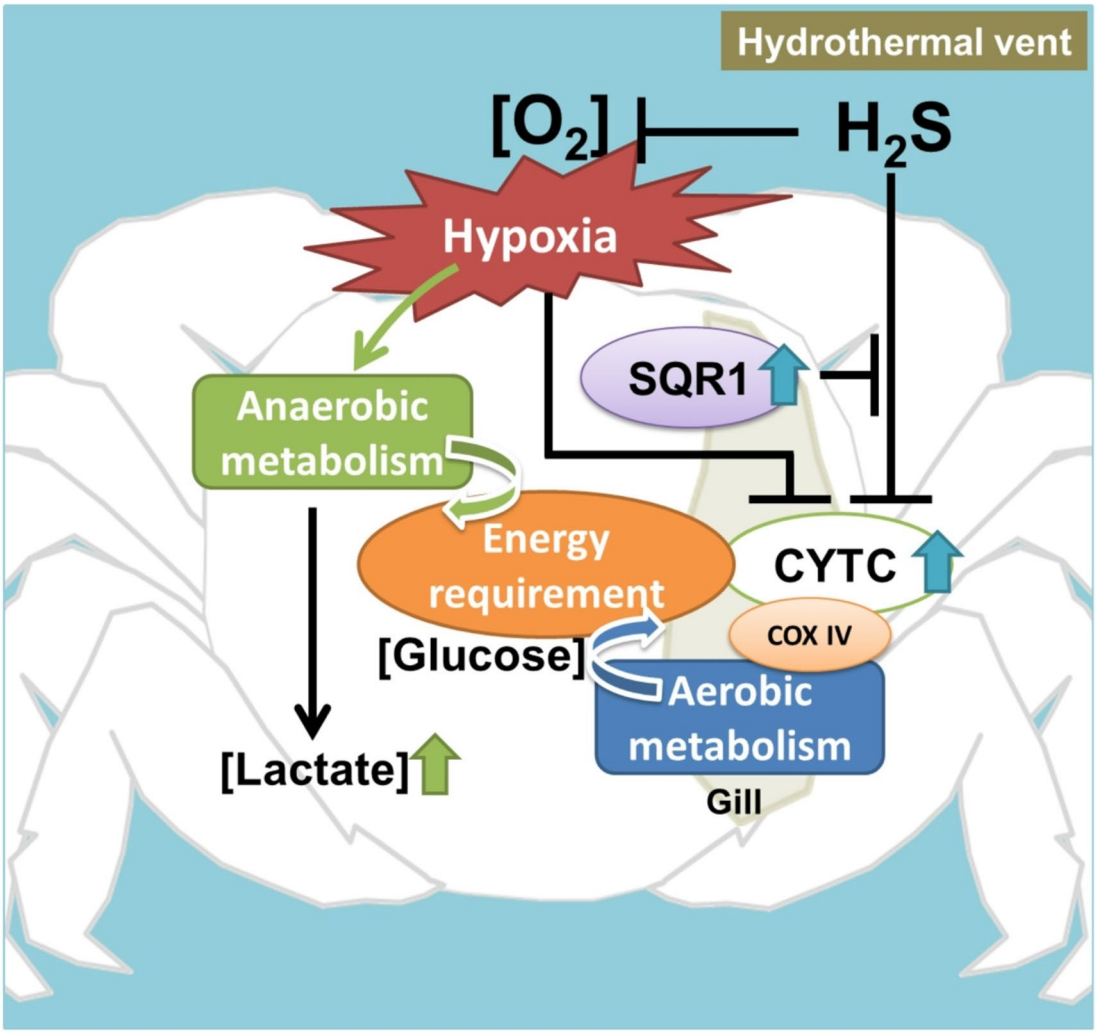

Fig. 7. Proposed physiological adaptation of *xt*crabs to high sulfide and low dissolved oxygen in hydrothermal vent environment. Hydrogen sulfide suppressed *xt*CYTC function which serves as the electron carrier between Complex III (cytochrome bc1 complex) and Complex IV (cytochrome c oxidase) in the mitochondria. Therefore, sulfide interrupts the electron transport chain and inhibit aerobic respiration. Additionally, the lack of O_2 directly decreases the activities of *xt*CYTC and aerobic respiration. To cope with high sulfide-hypoxia ecological niches, *xt*SQR in *xt*crab gills are labored for sulfide detoxification and also favored for mitochondrial electron transport chain. Moreover, the increased *xtCYTC* transcripts may recruit the reduced state of *xt*CYTC protein to replace sulfide-induced oxidized state of *xt*CYTC. Hydrogen sulfide easily interacts with the ambient oxygen and then induces a hypoxic environment[14]. The increase in anaerobic metabolism is rapidly turning on to cope with the decreased energy production from aerobic respiration in ecological niches with lower O_2. Meanwhile, vent *xt*crabs also try to keep the operation of aerobic metabolism and maintain a certain degree of aerobic respiration (as shown with a similar *xt*COXIV enzymatic activities between habitat *xt*crabs and aquarium *xt*crabs). These multiple strategies may contribute to the acclimation and adaptation of *xt*crabs to the hydrothermal vent extreme environment.

By integrating ecological, physiological, and molecular approaches, we found that *X. testudinatus* employs both aerobic and anaerobic pathways concurrently. The ability to rapidly switch to anaerobiosis ensures a continuous energy supply under fluctuating oxygen and sulfide levels. Collectively, these findings suggest that multiple metabolic strategies support the acclimation, adaptation, and survival of *X. testudinatus* in the extreme, sulfide-rich, hypoxic conditions of shallow-water hydrothermal vents.

Methods

Crab collection and sampling

Vent *xt*crabs were collected from the hydrothermal vent region in Kueishan Island, Taiwan by SCUBA divers (station-1, 24°50′31″N, 121°57′6″E) during 2016–2022 (Fig. 3, Table S1). The individual carapace lengths widths ranged from 15 to 25 mm. Sampled vent *xt*crabs were either (i) immediately submerged and anesthetized with 120 μM eugenol in seawater (referred to as "habitat *xt*crabs"), hemolymph was collected and posterior gill (pGi) were sampled, (ii) dissected for hemolymph and pGi sampling during field transfer experiment, (iii) maintained in seawater on the boat and transferred to aquaria laboratory at National Taiwan Ocean University (NTOU; referred to as "aquarium *xt*crabs"). For comparison, intertidal crabs (control species crab), *Thranita danae* (*td*crab, Portunidae), were collected by net from the intertidal zone of a rocky seashore in Keelung coast, Taiwan in 2019, 2022 and 2022 (25°08′09.1″N, 121°48′10.4″E; Fig. 3). The individual sizes ranged from 25 to 35 mm in carapace length and from 50 to 60 mm in carapace width and were transferred to aquaria at NTOU. Aquarium *xt*crabs and *td*crabs were held in a respectively 300 L tank with normal seawater and daylight conditions for one month. Crabs were fed with the shrimp food pellets (Omega, Kaohsiung, Taiwan) once a day. The collected samples were frozen in liquid nitrogen and then kept at −80℃ freezer in the field and laboratory experiments.

Field transfer experiment

To discover the aerobic and anaerobic metabolism of aquarium *xt*crabs encountered the hydrothermal vent environment, two sets of aquarium *xt*crabs (n = 6) in the 60 × 25 × 25 cm plastic cage (n = 6 crabs/group/cage) were left at transfer stations (depth = 9 m) for 2 hr. One group of aquarium *xt*crabs (n = 6) were transferred back to the hydrothermal vent region of Kueishan Island with a plastic cage (sulfide-rich environment, station-1 24°50′31″N, 121°57′6″E; Fig. 3, Table S1) and were referred to as "station-1 *xt*crabs." Another group of the aquarium *xt*crabs (n = 6) were transferred to non-hydrothermal vent region of Kueishan Island with a plastic cage (sulfide-free environment of normal seawater, station-2: 24°50′558″N, 121°56′212″E; Fig. 3) and were referred to as "station-2 *xt*crabs." After transfer experiment, the cages were collected, and the experimental crabs were collected for hemolymph samples to analyze hemolymph glucose and lactate levels. For further comparison, "habitat *xt*crabs" were sacrificed at various intervals after transfer to normal seawater (10 min, 30 min, 60 min, 6 h, 12 h, and 1 month) for the collection of hemolymph and analysis of lactate and glucose levels.

Tissue sampling

For tissue sampling, all experimental crabs were submerged in seawater containing 120 μM eugenol for anesthesia. Before sampling, the crabs were recorded for the length of the carapace. For tissue distributions of cytochrome c (*xtCYTC* transcripts by qPCR), habitat *xt*crabs (n = 6) and aquarium *xt*crabs (n = 6) were analyzed; tissues including anterior gills (aGi), posterior gills (pGi), stomach (St), digestive gland (DG), intestine (In), muscle (Mu), and heart (He) according to previous study[14]. pGi from 36 habitat *xt*crabs and 36 aquarium *xt*crabs were obtained from our previous study further analyze the *xt*CYTC transcripts by qPCR[14]. To analyze the *xtSQR1* transcripts by qPCR, pGi from 10 habitat *xt*crabs and 10 aquarium *xt*crabs were collected. To analyze the COXIV enzymatic activity, pGi of 6 habitat *xt*crabs and 6 aquarium *xt*crabs were collected. To analyze the SQR enzymatic activity, pGi of 3 habitat *xt*crabs, 3 aquarium *xt*crabs, and 3 control *td*crabs were collected. To analyze the Western blot and immunofluorescence of *xt*CYTC, 3 habitat *xt*crabs and 3 aquarium *xt*crabs were collected.

Severe hypoxic experiment

Habitat *xt*crabs and *td*crabs were subjected to a hypoxic challenge. The hypoxic environments in the aquarium (direct infusion with nitrogen gas for 30 min continuously flushing from DO = 8.31 mg/L to DO = 0.19 mg/L), was prepared by continuously flushing with nitrogen gas for 24 h in the 2 L aquarium at 25 ℃ with thermostat. An Orion Star™ A329 Portable pH/ISE/Conductivity/DO meter (Thermo Fisher Scientific, Waltham, MA, USA) was used to monitor the DO valu[14]. Survival was checked every 4 h using several indicators to evaluate the activity of crabs as described in previous study[14]. During the hypoxic exposure, hemolymph samples were independently collected at 0, 1, 3, 6, and 12 h (n = 8 *xt*crabs/group and n = 4 *td*crabs/group for each time point) and used for the analysis of lactate and glucose contents.

Cellular hypoxia induced by antimycin A

Antimycin A is a potent inhibitor of the mitochondrial electron transport chain and is used to induce cellular hypoxia[27,28]. To test the tolerance of *xt*crabs to chemical induced hypoxia, antimycin A (A8674, Sigma-Aldrich, St. Louis, MO, USA) exposure experiment was conducted with aquarium *xt*crabs. To investigate the tolerance to hypoxia and 50% lethal concentration (LC_{50}) during 96 h in *xt*crabs, several antimycin A concentrations (from 0 ppm up to high dose) were tested (0 ppb, 1 ppb, 10 ppb, 100 ppb, 500 ppb, and 1000 ppb) for 96 h in 2 L aquaria at 25 ℃. Survivals, as described previously, was recorded every 24 h (n = 9 crabs/treatment). The 50% lethal concentration (LC_{50}) of antimycin A was calculated at 96 h.

Measurement of oxygen consumption

To assess the impact of antimycin A on metabolism, oxygen consumption was measured under different concentrations of antimycin A. Before the experiment, seawater was filtered with the 0.22 μm filter to remove the bacterial respiration effect. Aquarium *xt*crabs were placed in sealed 500 ml glass chambers with different antimycin A concentrations: 0 ppb, 40 ppb, 120 ppb, 160 ppb, 200 ppb, and 400 ppb. Each chamber contained one crab and three-repeated independent test were performed (n = 3 crabs/group). The oxygen consumption rate was monitored by using the OXY-4 mini-multichannel fiber optic oxygen transmitter (PreSens, Regensburg, Germany). The device set-up followed the manufacturer's instructions (https://www.presens.de/products/detail

/oxy-4-mini). For calibration, 0% standard was made with 1% $NaHSO_3$ (243973, Sigma-Aldrich) seawater, and 100% standard was made with 30 min air pumped seawater. A chamber with only filtered seawater was used as the background control. During the experiment, the temperature was maintained at 25 ℃. To achieve the optimal measurement time, the oxygen consumption of individuals was measured until the air saturation level dropped to 80%. To obtain the mass-specific oxygen consumption rates, the wet weight was recorded and the oxygen consumption rate (mg O_2 g^{-1} hr^{-1}) was calculated[52].

Measurement of lactate and glucose levels in hemolymph

The hemolymph samples (100 µl) collected from the nitrogen-induced hypoxia experiment and field transfer experiment were used for the analysis of lactate and glucose content. After the collection of hemolymph, samples were centrifuged to 1,000 rpm at 4℃ for 5 min to remove particles. Lactate and glucose levels were detected using the L-Lactate Assay Kit (ab65330, Abcam, Cambridge, MA, USA) and Glucose Assay Kit (MAK263, Sigma-Aldrich) according to the manufacturer's instructions, respectively.

Cloning of *xt*crab *cytochrome c* (*CYTC*) cDNA

Posterior gill samples (pGi), which were used to build our in-house transcriptome of *xt*crab, were homogenized in TRIzol reagent (Invitrogen, Waltham, MA, USA). Total RNA was extracted following the manufacturer's protocol. The quality and quantity of total RNA was determined by gel electrophoresis and NanoDrop™ 1000 spectrophotometer (Thermo Fisher Scientific, Waltham, MA, USA), respectively. Total RNA extracts were used for Illumina sequencing, cDNA library construction, and cDNA synthesis.

For RNA-seq, total RNA extracts were performed by Genomics, Inc. (New Taipei city, Taiwan). Paired-end sequencing (150 bp) was performed on a HiSeq 2500 (Illumina, San Diego, CA, USA). Raw reads were uploaded to the Galaxy platform (http://usegalaxy.org) for cDNA library construction. Trimmed reads were generated from raw reads using the Trimmomatic trimming tool (ILLUMINACLIP step, Slide Window = 4:5, Leading = 5, Trailing = 5, minlen = 25) by removing adapters and low-quality reads. All trimmed reads were pooled together for *de novo* assembly by Trinity (v2.9.1) to get the assemble transcripts dataset as our cDNA library (SRR33664475). Assemble transcripts were used as a local BLAST database to design the primers for gene cloning. Primers are listed (Table S2).

For cDNA synthesis, pGi was homogenized in Trizol reagent (Invitrogen, Waltham, MA, USA). Total RNA was extracted according to manufacturer's protocol. The first-stand cDNA was synthesized from 1 µg total RNA by Superscript III reverse transcriptase (Invitrogen, Waltham, MA, USA) according to the manufacturer's protocol. Full-length (including ORF) of *xtCYTC* was found and cloned in gill[14].

Cloning of *TdSQRs*

The two paralogs of *xt*crab SQR were cloned in our previous study[14]. For comparison, posterior gill samples collected from *td*crabs were used for RNA extraction and cDNA synthesis following the manufacturer's protocol. The SQR partial sequences in *td*crabs, *tdSQR1* and *tdSQR2* which derived from our previous study[14] were used as templates to obtain the full length with a rapid amplification of cDNA ends (RACE) kit (SMART RACE cDNA; BD Biosciences Clontech, Franklin Lakes, NJ, USA) (Table S1). The sequence alignment and the identity between SQR paralogs were analyzed with DNAMAN sequence analysis software.

Phylogenetic analyses of CYTC and SQR sequences

The amino-acid sequences of CYTC from various species including full-length of *xt*CYTC were automatically aligned with MUSCLE, as implemented in Mega11[53]. The phylogenetic tree was constructed using the neighbor-joining method with the best model (LG + G, Gamma rate = 0.6178) in MEGA11[53]. The number at each node represents the bootstrap value (% from 1000 replicates). The accession numbers of the sequences used in the analysis are listed (Table S3).

The amino-acid sequences of SQR from various species including full-length of *xt*SQR paralogs and *td*SQR paralogs were aligned and the phylogenetic tree was constructed as described above for CYTC. The accession numbers of the sequences used in the analysis are listed (Table S4).

qPCR analyses of *XtCYTC* and *xtSQR1*

The quantitative real-time PCR (qPCR) was used to analyze the gene expression profiles. *Elongation factor 1 alpha* (*EF1A*) was used as an internal reference to normalize gene expression levels. We developed *xtCYTC* and *xtSQR1* qPCR analysis according to previous study[14]. The data were calibrated according to the $2^{-\Delta\Delta}$Ct method[54]. The relative expression value of target gene in all samples was normalized to *EF1A*, and the highest value of the target gene was defined as 100%. Specific primers for *xt*SQR1, *xtCYTC* and *xtEF1A* were listed (Table S2).

Enzymatic activities of SQR and COXIV in *xt*crabs and *td*crabs

SQR is suggested as an important enzyme for the detoxification of vent sulfide in *xt*crabs[14]. We measured SQR enzyme in the pGi mitochondria of *xt*crab and *td*crabs. Mitochondria were isolated and the SQR enzymatic activity assay was performed according to our previous study[14].

COXIV is considered as an important factor for the aerobic respiration involving electron chain transport. *xt*COXIV enzymatic activities in the isolated mitochondria were detected using the cytochrome c oxidase assay kit (ab239711, Abcam).

The production of *xt*CYTC and *xt*SQR antisera

A polyclonal anti-*xt*CYTC antisera was induced against to the synthetic peptide (CAQCHTVEAGGKHKTGPN). The synthetic peptide was conjugated with ovalbumin (OVA) and used to immunize the antisera. The preparation

of antisera was conducted by commercial company (Yao-Hong Biotechnology, Inc., New Taipei, Taiwan). After the synthetic peptide immunization, the sera from the mice were collected for Western blot analysis and immunofluorescence staining.

A polyclonal anti-*xt*SQR antisera was induced against to the synthetic peptide (SPKHQYDGYTSCPLVTGYSKCIMAEFDMNLS). The synthetic peptide was conjugated with ovalbumin (OVA) and used to immunize the antisera. The antiserum was purified using an affinity column containing 3 mg of synthetic peptide (Yao-Hong Biotechnology Inc.). The purified antibody was used for Western blot analysis and immunofluorescence staining.

*xt*CYTC Western blot analysis

The protein extraction, protein concentration determination, and Western blot (WB) analysis of the posterior gills were performed as our previous study[14]. To validate the antisera specificity, the synthetic *xt*CYTC peptide (1 µg per ml 1.5% nonfat milk) were incubated with anti-*xt*CYTC (diluted 1:1,000 with 1.5% nonfat milk) at 37℃ for 1 h as preadsorption reaction WB analysis. To detect the CYTC and Actin proteins, mouse anti-*xt*CYTC (diluted 1:1,000 with 1.5% nonfat milk) and mouse anti-human Actin antibody (MAB1501, Merck, Darmstadt, Germany; diluted 1:10,000 with 1.5% nonfat milk) were used. For secondary antibody, alkaline phosphate-conjugated goat anti-mouse IgG antibody (31320, Thermo Fisher Scientific; diluted 1:10,000 with 1.5% nonfat milk) were used. For detection, the NBT/BCIP Detection System (B1911, Sigma-Aldrich, St. Louis, MO, USA) was used. The same procedures of specificity validation were conducted with the anti-SQR antibody (diluted 1:1,000 with 1.5% nonfat milk).

Immunofluorescence staining

The tissue fixation, paraffin embedding, antigen retrieval, and immunofluorescence staining of the posterior gills were performed as our previous study[14]. DAPI (DAPI; 4', 6-diamidino-2-phenylindole; Vector Laboratories, Burlingame, CA, USA) was used to label the nuclear DNA in all staining. For co-staining of SQR and Na^+/K^+-ATPase (NKA), the rabbit anti-SQR antibody (diluted 1:200 with 1.5% nonfat milk powder) and the mouse anti-NKA antibody (Developmental Studies Hybridoma Bank, Iowa city, IA, USA; diluted 1:200 with 1.5% nonfat milk powder) were used. Secondary antibodies of Alexa Fluor 488-conjugated goat anti-rabbit IgG (H + L) (A-11034, Thermo Fisher Scientific; diluted 1:200 with 1.5% nonfat milk powder) and Alexa Fluor 546-conjugated goat anti-mouse IgG (H + L) (A-11030, Thermo Fisher Scientific; diluted 1:200 with 1.5% nonfat milk powder) were used for the detection of anti-*xt*SQR and anti-NKA primary antibodies, respectively. For co-staining of *xt*SQR and *xt*CYTC, the rabbit anti-*xt*SQR antibody (diluted 1:200 with 1.5% nonfat milk powder) and the mouse anti-*xt*CYTC antisera (diluted 1:200 with 1.5% nonfat milk powder) were used. Secondary antibodies of Alexa Fluor 488-conjugated goat anti-mouse IgG (H + L) (A-11029, Thermo Fisher Scientific; diluted 1:200 with 1.5% nonfat milk powder) and Alexa Fluor 546-conjugated goat anti-rabbit IgG (H + L) (A-11035, Thermo Fisher Scientific; diluted 1:200 with 1.5% nonfat milk powder) were used for the detection of anti-*xt*CYTC antisera and anti-*xt*SQR primary antibody, respectively. All signals in the cells of the gill were observed, and images were captured under fluorescence microscopy (Olympus BX53).

Data analysis

Data are shown as mean ± standard deviation (SD). One-way ANOVA followed by a Tukey's analysis was performed with Statistical Package for the Social Science (SPSS) software to test the significance of differences among three or more groups. Student's *t*-test was used to analyze the significance of differences between two groups. Asterisks ($p < 0.05$: *, $p < 0.01$: **, $p < 0.001$: ***) indicate significant difference.

Data availability

The original data are available from Chi Chen and Ching-Fong Chang upon requests.

Received: 4 September 2025; Accepted: 5 December 2025
Published online: 15 December 2025

References

1. Wannamaker, C. M. & Rice, J. A. Effects of hypoxia on movements and behavior of selected estuarine organisms from the southeastern united States. *J. Exp. Mar. Biol. Ecol.* **249** (2), 145–163. https://doi.org/10.1016/s0022-0981(00)00160-x (2000).
2. Giomi, F. & Beltramini, M. The molecular heterogeneity of hemocyanin: its role in the adaptive plasticity of crustacea. *Gene* **398** (1–2), 192–201. https://doi.org/10.1016/j.gene.2007.02.039 (2007).
3. McMahon, B. R. Respiratory and circulatory compensation to hypoxia in crustaceans. *Respir Physiol.* **128** (3), 349–364. https://doi.org/10.1016/S0034-5687(01)00311-5 (2001).
4. de Lima, T. M., Geihs, M. A., Nery, L. E. M. & Maciel, F. E. Air exposure behavior of the semiterrestrial crab Neohelice granulata allows tolerance to severe hypoxia but not prevent oxidative damage due to hypoxia–reoxygenation cycle. *Physiol. Behav.* **151**, 97–101. https://doi.org/10.1016/j.physbeh.2015.07.013 (2015).
5. de Lima, T. M. et al. Emersion behavior of the semi-terrestrial crab Neohelice granulata during hypoxic conditions: Lactate as a trigger. *Comp Biochem Physiol A Mol Integr Physiol*, 252, 110835. (2021). https://doi.org/10.1016/j.cbpa.2020.110835 (2021).
6. Hirota, S. et al. Structural basis of the lactate-dependent allosteric regulation of oxygen binding in arthropod Hemocyanin. *J. Biol. Chem.* **285** (25), 19338–19345 (2010).
7. Van Dover, C. L. *The Ecology of deep-sea Hydrothermal Vents* (Princeton University Press, 2000). https://doi.org/10.1515/9780691239477
8. Powell, M. & Somero, G. Adaptations to sulfide by hydrothermal vent animals: sites and mechanisms of detoxification and metabolism. *Biol. Bull.* **171** (1), 274–290 (1986).
9. Chiu, L. et al. Shallow-water hydrothermal vent system as an extreme proxy for discovery of Microbiome significance in a crustacean holobiont. *Front. Mar. Sci.* 1670. https://doi.org/10.3389/fmars.2022.976255 (2022).

10. Sun, Y. et al. Adaption to hydrogen sulfide-rich environments: strategies for active detoxification in deep-sea symbiotic mussels, Gigantidas platifrons. *Sci. Total Environ.* **804**, 150054. https://doi.org/10.1016/j.scitotenv.2021.150054 (2022).
11. Mickel, T. J. & Childress, J. J. Effects of temperature, pressure, and oxygen concentration on the oxygen consumption rate of the hydrothermal vent crab bythograea thermydron (Brachyura). *Physiol. Zool.* **55** (2), 199–207 (1982).
12. Sanders, N. & Childress, J. Specific effects of thiosulphate and L-lactate on hemocyanin-O_2 affinity in a brachyuran hydrothermal vent crab. *Mar. Biol.* **113** (2), 175–180. https://doi.org/10.1007/BF00347269 (1992).
13. Jeng, M. S., Ng, N. & Ng, P. Hydrothermal vent crabs feast on sea 'snow'. *Nature* **432** (7020), 969–969. https://doi.org/10.1038/432969a (2004).
14. Chen, C. et al. Duplicated paralog of sulfide: Quinone oxidoreductase contributes to the adaptation to hydrogen sulfide-rich environment in the hydrothermal vent crab, xenograpsus testudinatus. *Sci. Total Environ.* **890**, 164257. https://doi.org/10.1016/j.scitotenv.2023.164257 (2023).
15. Corrigan, E., Chen, C. J., Wang, B. S., Dufour, S. & Chang, C. F. Robustness of gametogenesis in the scleractinian coral, Tubastraea aurea, in the shallow-water hydrothermal vent field off Kueishan Island, Northeastern Taiwan. *Sci. Total Environ.* **992**, 179901. https://doi.org/10.1016/j.scitotenv.2025.179901 (2025).
16. Chan, B. K. K. et al. Community structure of macrobiota and environmental parameters in shallow water hydrothermal vents off Kueishan Island, Taiwan. *PLoS One.* **11** (2), e0148675. https://doi.org/10.1371/journal.pone.0148675 (2016).
17. Mei, K. et al. Transformation, fluxes and impacts of dissolved metals from shallow water hydrothermal vents on nearby ecosystem offshore of Kueishantao (NE Taiwan). *Sustainability* **14** (3), 1754. https://doi.org/10.3390/su14031754 (2022).
18. Wang, Y. G. et al. Copepods as indicators of different water masses during the Northeast monsoon prevailing period in the Northeast Taiwan. *Biology* **11** (9), 1357. https://doi.org/10.3390/biology11091357 (2022).
19. Chiu, L., Wang, M. C., Wei, C. L., Lin, T. H. & Tseng, Y. C. A two-year physicochemical and acoustic observation reveals Spatiotemporal effects of earthquake-induced shallow-water hydrothermal venting on the surrounding environments. *Limnol. Oceanogr. Lett.* **9** (4), 423–432. https://doi.org/10.1002/lol2.10412 (2024).
20. Davidson, A. M., Tseng, L. C., Wang, Y. G. & Hwang, J. S. Mortality of mesozooplankton in an acidified ocean: investigating the impact of shallow hydrothermal vents across multiple monsoonal periods. *Mar. Pollut Bull.* **205**, 116547. https://doi.org/10.1016/j.marpolbul.2024.116547 (2024).
21. Huang, Y. H. & Shih, H. T. Diversity of the swimming crabs (Crustacea: brachyura: Portunidae) from Dongsha Island, with a new record from Taiwan. *J. Taiwan. Mus.* **76** (3&4), 37–102. https://doi.org/10.6532/JNTM.202312_76(3_4).04 (2023).
22. Jansen, S. et al. Functioning of intertidal flats inferred from Temporal and Spatial dynamics of O_2, H_2S and pH in their surface sediment. *Ocean. Dyn.* **59** (2), 317–332 (2009).
23. Nicholls, P. & Kim, J. K. Sulphide as an inhibitor and electron donor for the cytochrome c oxidase system. *Can. J. Biochem.* **60** (6), 613–623. https://doi.org/10.1139/o82-076 (1982).
24. Khan, A. et al. Effects of hydrogen sulfide exposure on lung mitochondrial respiratory chain enzymes in rats. *Toxicol. Appl. Pharmacol.* **103** (3), 482–490. https://doi.org/10.1016/0041-008x(90)90321-k (1990).
25. Searcy, D. G. Metabolic integration during the evolutionary origin of mitochondria. *Cell. Res.* **13** (4), 229–238. https://doi.org/10.1038/sj.cr.7290168 (2003).
26. Vitvitsky, V. et al. Cytochrome c reduction by H_2S potentiates sulfide signaling. *ACS Chem. Biol.* **13** (8), 2300–2307. https://doi.org/10.1021/acschembio.8b00463 (2018).
27. Morrison, B. R. S. An investigation into the effects of the piscicide antimycin A on the fish and invertebrates of a Scottish stream. *Aquac Res.* **10** (3), 111–122. https://doi.org/10.1111/j.1365-2109.1979.tb00262.x (1979).
28. Han, Y. H., Kim, S. H., Kim, S. Z. & Park, W. H. Antimycin A as a mitochondrial electron transport inhibitor prevents the growth of human lung cancer A549 cells. *Oncol. Rep.* **20** (3), 689–693. https://doi.org/10.3892/or_00000061 (2008).
29. 29. Shahak, Y & Hauska, G. Sulfide Oxidation from Cyanobacteria to Humans: Sulfide–Quinone Oxidoreductase (SQR) in Sulfur Metabolism in Phototrophic Organisms. Advances in Photosynthesis and Respiration (ed. Hell, R., Dahl, C., Knaff, D & Leustek, T.) vol 27. Springer, Dordrecht. https://doi.org/10.1007/978-1-4020-6863-8_16(2008).
30. Marcia, M., Ermler, U., Peng, G. & Michel, H. A new structure-based classification of sulfide: Quinone oxidoreductases. *Proteins* **78** (5), 1073–1083. https://doi.org/10.1002/prot.22665 (2010).
31. Hu, M. Y. et al. Strong ion regulatory abilities enable the crab xenograpsus testudinatus to inhabit highly acidified marine vent systems. *Front. Physiol.* **7**, 14. https://doi.org/10.3389/fphys.2016.00014 (2016).
32. Diaz, R. J. & Rosenberg, R. Spreading dead zones and consequences for marine ecosystems. *Science* **321** (5891), 926–929. https://doi.org/10.1126/science.1156401 (2008).
33. Isensee, K. et al. The ocean is losing its breath. In Ocean and Climate Scientific Notes. Vol. 2. 20–32 (2016). (2016).
34. Arp, A. J. & Childress, J. J. Functional characteristics of the blood of the deep-sea hydrothermal vent brachyuran crab. *Science* **214** (4520), 559–561. https://doi.org/10.1126/science.214.4520.559 (1981).
35. Fredricks, K. T., Hubert, T. D., Amberg, J. J., Cupp, A. R. & Dawson, V. K. Chemical controls for an integrated pest management program. *N Am. J. Fish. Manag.* **41** (2), 289–300. https://doi.org/10.1002/nafm.10339 (2021).
36. Ott, K. C. & Antimycin A brief review of it's chemistry, environmental fate, and toxicology. *Biochem. Et Biophys. Acta*. **1185**, 1–9 (1994).
37. Saari, G. N. Antimycin-A species sensitivity distribution: perspectives for non-indigenous fish control. *Manag Biol Invasions.* 14(3). https://doi.org/%2010.3391/mbi.14.3.09 (2023). (2023).
38. Thorpe, K. E., Taylor, A. C. & Huntingford, F. A. How costly is fighting? Physiological effects of sustained exercise and fighting in swimming crabs, Necora puber (L.)(Brachyura, Portunidae). *Anim. Behav.* **50** (6), 1657–1666. https://doi.org/10.1016/0003-3472(95)80019-0 (1995).
39. Cota-Ruiz, K., Peregrino-Uriarte, A. B., Felix-Portillo, M., Martnez-Quintana, J. A. & Yepiz-Plascencia, G. Expression of Fructose 1, 6-bisphosphatase and phosphofructokinase is induced in hepatopancreas of the white shrimp Litopenaeus vannamei by hypoxia. *Mar. Environ. Res.* **106**, 1–9. https://doi.org/10.1016/j.marenvres.2015.02.003 (2015).
40. Reyes-Ramos, C. A. et al. Phosphoenolpyruvate Carboxykinase cytosolic and mitochondrial isoforms are expressed and active during hypoxia in the white shrimp Litopenaeus vannamei. *Comp. Biochem. Physiol. B Biochem. Mol. Biol.* **226**, 1–9. https://doi.org/10.1016/j.cbpb.2018.08.001 (2018).
41. Bao, J., Li, X., Yu, H. & Jiang, H. Respiratory metabolism responses of Chinese mitten crab, eriocheir sinensis and Chinese grass shrimp, palaemonetes sinensis, subjected to environmental hypoxia stress. *Front. Physiol.* **9**, 1559. https://doi.org/10.3389/fphys.2018.01559 (2018).
42. Opie, L. H. & Lopaschuk, G. D. *Fuels: Aerobic and Anaerobic metabolism. Heart Physiology: from Cell To Circulation* 4th edn, 306–354 (Lippincott, Williams and Wilkins, 2004).
43. Hervant, F., Garin, D., Mathieu, J. & Freminet, A. Lactate metabolism and glucose turnover in the subterranean crustacean niphargus virei during post-hypoxic recovery. *J. Exp. Biol.* **202** (5), 579–592. https://doi.org/10.1242/jeb.202.5.579 (1999).
44. Kabil, O. & Banerjee, R. Redox biochemistry of hydrogen sulfide. *J. Biol. Chem.* **285** (29), 21903–21907. https://doi.org/10.1074/jbc.R110.128363 (2010).
45. Kelly, J. L. et al. Mechanisms underlying adaptation to life in Hydroten sulfide-rich environments. *Mol. Biol. Evol.* **33** (6), 1419–1434. https://doi.org/10.1093/molbev/msw020 (2016).

46. Henry, R. P., Lucu, C., Onken, H. & Weihrauch, D. Multiple functions of the crustacean gill: osmotic/ionic regulation, acid-base balance, ammonia excretion, and bioaccumulation of toxic metals. *Front. Physiol.* **3**, 431. https://doi.org/10.3389/fphys.2012.00431 (2012).
47. Ogunbona, O. B. & Claypool, S. M. Emerging roles in the biogenesis of cytochrome c oxidase for members of the mitochondrial carrier family. *Front. Cell. Dev. Biol.* **7**, 3. https://doi.org/10.3389/fcell.2019.00003 (2019).
48. Herzig, R. P., Scacco, S. & Scarpulla, R. C. Sequential serum-dependent activation of CREB and NRF-1 leads to enhanced mitochondrial respiration through the induction of cytochrome c. *J. Biol. Chem.* **275** (17), 13134–13141. https://doi.org/10.1074/jbc.275.17.13134 (2000).
49. Jimenez-Gutierrez, L. R., Uribe-Carvajal, S., Sanchez-Paz, A., Chimeo, C. & Muhlia-Almazan, A. The cytochrome c oxidase and its mitochondrial function in the whiteleg shrimp Litopenaeus vannamei during hypoxia. *J. Bioenerg Biomembr.* **46**, 189–196. https://doi.org/10.1007/s10863-013-9537-5 (2014).
50. Pfenninger, M. et al. Parallel evolution of Cox genes in H_2S-tolerant fish as key adaptation to a toxic environment. *Nat. Commun.* **5** (1), 3873. https://doi.org/10.1038/ncomms4873 (2014).
51. Mellado, M., de Ana, A. M., Moreno, M. C., Martínez-A, C. & Rodrıguez-Frade, J. M. A potential immune escape mechanism by melanoma cells through the activation of chemokine-induced T cell death. *Curr. Biol.* **11** (9), 691–696. https://doi.org/10.1016/s0960-9822(01)00199-3 (2001).
52. Shi, Y. et al. Effects of salinity on survival, growth, haemolymph osmolality, gill Na+-K+-ATPase activity, respiration and excretion of the sword Prawn *Parapenaeopsis hardwickii*. *Aquac Res.* **53** (2), 603–611. https://doi.org/10.1111/are.15604 (2022).
53. Kumar, S., Stecher, G. & Tamura, K. MEGA7: molecular evolutionary genetics analysis version 7.0 for bigger datasets. *Mol. Biol. Evol.* **33** (7), 1870–1874. https://doi.org/10.1093/molbev/msw054 (2016).
54. Livak, K. J. & Schmittgen, T. D. Analysis of relative gene expression data using real-time quantitative PCR and the 2(-Delta delta C(T)) method. *Methods* **25** (4), 402–408. https://doi.org/10.1006/meth.2001.1262 (2001).

Acknowledgements

This work was supported by the Center of Excellence for the Oceans, NTOU from The Featured Areas Research Center Program within the framework of the Higher Education Sprout Project by the Ministry of Education (MOE), Taiwan, the Yushan Scholar Program (Sylvie Dufour), MOE, Taiwan (MOE-113-YSFAG-0012-001-P2), and the National Science and Technology Council (NSTC 112-2313-B-019-008; 113-2313-B-019-014). We thank to captain Dai-Shiu Lan, SCUBA diving coach Jen-Wei Lu, and Jen-sheng Lu for xtcrabs collection. We thank the staff of Yung-Che Tseng's laboratory at Academia Sinica for xtcrabs collection. We thank Ying-Syuan Lyu of Ching-Fong Chang's laboratory at NTOU for xtcrabs collection. We thank Emily Corrigan for the English correction. Thanks to Jie-Lin Guo of Ching-Fong Chang's laboratory at NTOU for tdcrabs collection.

Author contributions

Chi Chen: conducted the sample collection, developed the methodologies in *xt* crab and *td* crab performed the experiments, data curation and analyses of data, and wrote the original draft. Guan-Chung Wu, Yung-Che Tseng and Ching-Fong Chang: developed the concept of the study, guided the experiments, and evaluated the data. Ching-Fong Chang: acquired funding, wrote, reviewed, and edited the paper. Sylvie Dufour: gave important input into conceptual and mechanistic insights, reviewed and edited the paper. All authors approved the paper.

Funding

This work was supported by the Center of Excellence for the Oceans, NTOU from The Featured Areas Research Center Program within the framework of the Higher Education Sprout Project by the Ministry of Education (MOE), Taiwan, the Yushan Scholar Program (Sylvie Dufour), MOE, Taiwan (MOE-113-YSFAG-0012-001-P2), and the National Science and Technology Council (NSTC 112-2313-B-019-008; 113-2313-B-019-014).

Declarations

Competing interests

The authors declare no competing interests.

Additional information

The online version contains supplementary material available at https://doi.org/10.1038/s41598-025-31968-1.

Correspondence and requests for materials should be addressed to C.C., G.-C.W. or C.-F.C.